A Moisture Analysis of the Meso β-Scale Thunderstorm Environment during AVE-SESAME V (20–21 May 1979)

HENRY E. FUELBERG,* YEONG-JER LIN AND HSIU-WU CHANG

Department of Earth and Atmospheric Sciences, Saint Louis University, St. Louis, MO 63103

(Manuscript received 28 February 1985, in final form 20 September 1985)

ABSTRACT

Meso β-scale radiosonde data at 75 km spacings and 3 or 1.5 h intervals from the fifth day of AVE-SESAME 1979 (20–21 May) are employed to investigate moisture budgets in thunderstorm environments. Budget values are computed at nine times prior to, during, and after a convective outbreak over Oklahoma. The domain under investigation includes both convective and nonconvective areas, thereby allowing budget comparisons between the two regions.

Findings show that the convective region is characterized by strong horizontal moisture flux convergence in the low levels and weak divergence aloft. Vertical motion carries moisture into the middle and upper troposphere. Magnitudes of the moisture fluxes are directly proportional to storm intensity. The vertically integrated source/sink term also is closely related to the presence and intensity of convective activity. When converted into equivalent precipitation amounts, values correspond closely with those from a rain gage network.

Moisture budgets also are obtained from routine National Weather Service rawinsonde soundings. A comparison of results for similar locations, but derived from the two different resolutions, reveals several common processes. However, magnitudes from the mesoscale data are sometimes an order of magnitude greater than those at the synoptic scale, especially in the convective areas.

1. Introduction

Water vapor content is one of the most important atmospheric parameters. When transformed into the liquid or solid phases, it provides life-sustaining precipitation. Furthermore, even if precipitation does not result, changes of phase affect the atmosphere because of latent heating. These processes must be incorporated into the numerical models. Since data at the appropriate scale generally are unavailable, the effects of convection usually are expressed in terms of relationships between the small-scale processes and measured parameters at larger scales, a procedure called parameterization.

Budget analyses of water vapor are a useful procedure for investigating its varying content. Studies based on synoptic-scale data include those of Spar (1953), Bradbury (1957), Hudson (1971), Thompson et al. (1979), and Bosart and Sanders (1981). The literature also contains budget results at mesoscale resolution (e.g., Fankhauser, 1969; Betts, 1973; Lewis, 1975; McNab and Betts, 1978; Sienkiewicz and Scoggins, 1982; Raymond and Wilkening, 1985). Furthermore, Fritsch et al. (1976) compared budgets based on mesoscale data with those from simultaneous synoptic-scale input. They found that a squall line consumed considerably more water vapor than was provided by synoptic-scale convergence, implying that smaller scale circulations were occurring. There have been few such comparison studies due to the lack of observations.

The purpose of this paper is to examine the water vapor budget of the mesoscale severe storm environment during the fifth day (20–21 May) of the 1979 Atmospheric Variability Experiment-Severe Environmental Storms and Mesoscale Experiment (AVE-SESAME V). Since radiosonde data are available at spacings of 75 km and intervals of 1.5–3 h, meso β-scale resolution (20–200 km) is provided (Orlanski, 1975). It should be stressed that our goal is to describe the storm environment, not individual convective elements. Budgets are examined prior to, during, and after a convective outbreak over Oklahoma in order to relate vapor fluctuations to storm activity. In addition, since data were collected simultaneously at the synoptic scale, we have a rare opportunity to compare results for the same analysis region derived from the two scales of resolution. The current paper is an extension of Fuelberg and Printy (1983, 1984), hereafter abbreviated FP, who examined the kinetic energy balance and various thunderstorm-environment interactions at the meso β and synoptic scales.

2. Methodology

a. Theoretical development

The continuity equation for water vapor in isobaric coordinates can be written as

* Present Affiliation: Department of Meteorology, Florida State University, Tallahassee, FL 32306.

$$\rho S = \rho\left(\frac{\partial q}{\partial t} + \nabla\cdot\mathbf{V}q + \frac{\partial \omega q}{\partial p}\right), \qquad (1)$$

where $\mathbf{V}$ is the horizontal wind vector, ω vertical velocity in isobaric coordinates, q specific humidity, ρ air density, and S sources and sinks of water vapor. If (1) is integrated in the vertical, and the hydrostatic assumption is made, one has

$$\underset{\mathrm{R}}{\frac{1}{g}\int_{p_2}^{p_1} S dp} = \underset{\mathrm{LC}}{-\frac{1}{g}\int_{p_2}^{p_1}\frac{\partial q}{\partial t}dp}$$

$$\underset{\mathrm{HF}}{-\frac{1}{g}\int_{p_2}^{p_1}\nabla\cdot\mathbf{V}q dp} \underset{\mathrm{VF}}{-\frac{1}{g}\int_{p_2}^{p_1}\frac{\partial \omega q}{\partial p}dp}, \qquad (2)$$

where term LC represents the local time change, while HF and VF denote horizontal and vertical moisture flux divergence/convergence, respectively. Here, R denotes the source/sink term representing the effects of evaporation, condensation and precipitation. It is computed as a residual to balance the other terms in (2). This formulation neglects the transport and storage of condensate, and a discussion of this aspect is provided in the results section.

b. Data and analysis procedure

During the fifth period of AVE-SESAME 1979, meso β-scale radiosonde data were gathered from 20 sites in Oklahoma and Texas (Fig. 1) at 3 h intervals between 1100 GMT 20 May and 1100 GMT 21 May. In addition, special 1.5 h soundings were taken at 2130 GMT 20 May, i.e., there were a total of 10 observation times. The average station spacing was approximately 75 km. In addition, 23 National Weather Service (NWS) sites surrounding the mesonetwork (Fig. 1) also collected data every 3 h. NWS soundings were not taken at 2130 GMT 20 May. The horizontal separation of these stations was approximately 400 km.

Analytical procedures applied to the data are identical to those of FP (1983, 1984). Since they provide complete descriptions, only highlights are presented herein. First, soundings were checked carefully to insure that they were representative of the storm environment where hydrostatic conditions were assumed. Data that appeared erroneous were deleted as necessary. Next, values at each level were adjusted to a common time using linear interpolation. Finally, the meso β-scale soundings were objectively analyzed onto a 15×13 grid of 25-km mesh by using the Barnes (1964) objective procedure. Sonde positions at individual levels were used instead of surface station locations. Analyses were obtained at the surface and at 50 mb intervals from 900 to 150 mb; however, one should note that humidity values were not reported above 350 mb. In order to suppress inherent errors, winds at individual

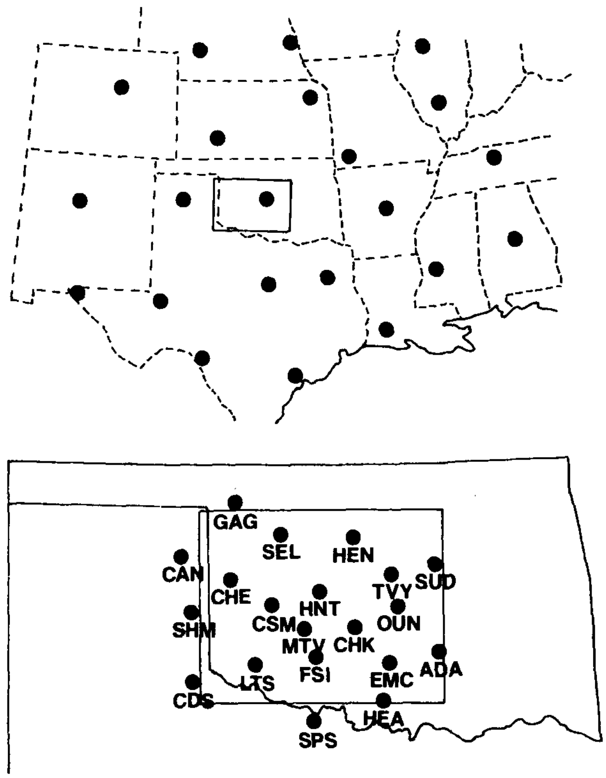

FIG. 1. Rawinsonde networks participating in the fifth day of AVE-SESAME 1979. The top diagram shows synoptic-scale sites, and the bottom gives the special network. The outline (bottom) indicates the meso β-scale domain under investigation which covers most of central and western Oklahoma.

50-mb levels were arithmetic averages of values at that level and those at 25 mb above and below. The final data grids have response values that are approximately 32% of originally resolved amplitudes at wavelengths of 150 km, and 82% at wavelengths of 225 km (two and three times the average station spacing). For the separate synoptic-scale calculations, the NWS rawinsonde data were objectively analyzed onto a grid having a 127 km spacing. Procedures were similar to those used for the mesoscale soundings; however, coarser resolution resulted, i.e., responses at wavelengths of 800 and 1200 km were approximately 65 and 90%, respectively. Both sets of grids have been utilized earlier by FP (1983, 1984).

The kinematic method was employed to compute vertical motion (ω). Profiles of ω were adjusted to zero at 150 mb using O'Brien's (1970) procedure. Corresponding modifications to horizontal divergence were a linear function of pressure. Except for uncentered 3 h differencing at the first observation time, temporal derivatives needed in (2) were obtained from a centered 6 h approach. No results are presented for the last time. At 2130 GMT, because of the 1.5 h data, the difference interval was only 3 h. Finally, both horizontal and verface–900 mb layer (Fig. 10). There is vertical flux convergence at the last two times at point G. Although mesoscale values are not consistently greater when the entire column is examined, vertical profiles (not shown) reveal uniformly greater mesoscale transport at individual levels. Finally, increasing humidity (positive LC) is evident from both scales of data at each time.

Variations and relative magnitudes of the residual at point G correspond to those of HF. Specifically, at 1700 GMT, both scales suggest a gain of vapor (negative values), and the mesoscale data continue this process through 2300 GMT. At the larger scale, on the other hand, the initally negative residual becomes positive by the end of the 6 h period, implying the condensation (loss) of vapor. Horizontal maps of R from the NWS network (not shown) indicate the development of a broad area of positive values over Texas and Oklahoma. Of course, the mesoscale data (Fig. 8) confined positive R to a much smaller region, thereby agreeing more closely with observed precipitation. Magnitudes of R are always greater at the mesoscale. It would be informative to determine whether the larger area of comparatively small positive residuals yielded the same equivalent total rainfall as the smaller area of greater values from the mesoscale data. Unfortunately, such an approach is not fruitful because the storms are not within the special network during their complete life cycles. As noted earlier, however, Fankhauser (1969) observed such a relationship between calculated rainfall on the mesoscale and a special network of dense rain gages. Furthermore, parameterization schemes have overestimated rain areas but underestimated peak amounts during major convective outbreaks (e.g., Lin and Smith, 1979; Fuelberg et al., 1985).

Contrasts between mesoscale and synoptic-scale budgets are more pronounced at point H (Table 2) where convective activity was very intense. The synoptic-scale data produce increasingly strong horizontal influx of vapor during the 6 h period. At the mesoscale, however, slight export dramatically changes to extreme flux convergence by 2300 GMT. One should note that the mesoscale value (-637×10^{-5} kg m^{-2} s^{-1}) is almost an order of magnitude greater than the corresponding synoptic-scale result (-77×10^{-5} kg m^{-2} s^{-1}). The residual exhibits predominantly positive values. Magnitudes at both the synoptic and mesoscale increase greatly during the 6 h interval of storm activity. At 2300 GMT, the mesoscale value is much larger than its synoptic-scale counterpart.

It is informative to compare values of HF and R (Table 2). Specifically, at 2300 GMT when convection near point H was very intense, mesoscale HF and R are nearly equal. Thus, to the extent that positive R represents the condensation and precipitation processes, it appears that horizontal influx of vapor is virtually the sole source. The same can be said for results at the larger scale. On the other hand, synoptic-scale horizontal influx is almost an order of magnitude smaller than ($\approx$12%) the mesoscale residual. Furthermore, within the surface–850 mb subcloud layer (not shown), synoptic-scale HF (-30×10^{-5} kg m^{-2} s^{-1}) is only about 6% of the mesoscale residual. Thus, current results are consistent with those of Fritsch et al. (1976) who found that synoptic-scale moisture convergence in the subcloud layer was about one-tenth of the mesoscale consumption rate.

Considering vertical transport (Table 2), mesoscale VF consistently exceeds values at the larger scale, sometimes by an order of magnitude. On the other hand, with the local derivative (LC), synoptic-scale values sometimes are greater than those from NWS soundings. Considering both G and H, it appears that contrasts between large- and small-scale values of LC generally are less than those of the other budget terms. This suggests that NWS data do a better job of resolving local changes in humidity than the transports and source/sink mechanisms from which those changes result.

6. Summary and conclusions

A meso β-scale water vapor budget analysis has been conducted for a period of intense convection that occurred over central Oklahoma during the 20–21 May day of AVE-SESAME 1979. Rawinsonde data at 75 km spacings and either 3 or 1.5 h intervals were used to examine moisture variations in the storm environment prior to, during, and after the convection.

Area-averaged results indicated that the meso β-scale storm environment was characterized by strong low-level horizontal moisture convergence, upward transport, and a positive residual representing the condensation and precipitation processes. Local changes of water vapor content were relatively minor. Values of the various terms were greatest during the time of most intense convection within the special network. The temporal variability and character of the various transports are consistent with previously investigated environmental variations near MCCs. Thus, we believe that they are attributable to feedback processes from the enclosed storms. For example, the enhanced low level flux convergence is due mostly to greater velocity convergence resulting from storm-induced latent heat release. On the other hand, this influx supplies the water vapor needed to sustain the storms. Thus, there is a cooperative interplay between the convection and its surrounding atmosphere.

Horizontal maps and cross sections revealed that budget processes were greatest near the storms. Patterns of the residual were especially interesting because they generally corresponded well with storm locations. Also, when converted to equivalent rainfall amounts, results compared favorably with observed values. This finding was especially encouraging in light of the term's greater uncertainty and our neglect of the transport and storage of condensate.

A unique feature of AVE-SESAME V is that rawinsonde data were collected simultaneously at both the synoptic and meso β-scales, making possible budget comparisons at the same point based on different scales of input data. Qualitatively, results from the two resolutions were often similar; however, near the storms, magnitudes at the mesoscale frequently approached an order of magnitude increase over the synoptic-scale values. Differences were especially pronounced for the residual and horizontal flux terms. Thus, as noted by Fritsch et al. (1976), large-scale data greatly underestimate water vapor budgets during convective activity.

Acknowledgments. The authors wish to thank Mr. Patrick Wright for performing many of the calculations and for assisting in figure preparation. Also, the anonymous reviewers offered several valuable suggestions for improvement. Finally, we appreciate the help of Ms. Rhonda Webb in typing the manuscript. This work was partially supported by the Division of Atmospheric Sciences of the National Science Foundation under NSF Grant ATM-8312172 to Dr. Y. J. Lin. Dr. H. E. Fuelberg was supported through NASA contract NAS8-35330 under the auspices of the Atmospheric Sciences Division, Systems Dynamics Laboratory, Marshall Space Flight Center, Alabama.

REFERENCES

Barnes, S. L., 1964: A technique for maximizing detail in numerical map analysis. *J. Appl. Meteor.,* **3,** 396–409.

Betts, A. K., 1973: A composite mesoscale cumulonimbus budget. *J. Atmos. Sci.,* **30,** 597–610.

Bosart, L. F., and F. Sanders, 1981: The Johnstown flood of July 1977: A long-lived convective system. *J. Atmos. Sci.,* **38,** 1616–1642.

Bradbury, D. L., 1957: Moisture analysis and water budget in three different types of storms. *J. Meteor.,* **14,** 559–565.

Chang, C. B., D. J. Perkey and C. W. Kreitzberg, 1982: A numerical case study of the effects of latent heating on a developing wave cyclone. *J. Atmos. Sci.,* **39,** 1555–1570.

——, —— and ——, 1984: Latent heat induced energy transformations during cyclogenesis. *Mon. Wea. Rev.,* **112,** 357–367.

Edmon, H. J., Jr., and D. G. Vincent, 1976: An application of two tropical parameterization schemes of convective latent heat release in middle latitudes. *Mon. Wea. Rev.,* **104,** 1141–1153.

Fankhauser, J. C., 1969: Convective processes resolved by a mesoscale rawinsonde network. *J. Appl. Meteor.,* **8,** 778–798.

Fritsch, J. M., and R. A. Maddox, 1981a: Convectively driven mesoscale weather systems aloft. Part I: Observations. *J. Appl. Meteor.,* **20,** 9–19.

——, and ——, 1981b: Convectively driven mesoscale weather systems aloft. Part II: Numerical simulations. *J. Appl. Meteor.,* **20,** 20–26.

——, and J. M. Brown, 1982: On the generation of convectively driven mesohighs aloft. *Mon. Wea. Rev.,* **118,** 1554–1565.

——, C. F. Chappell and L. R. Hoxit, 1976: The use of large-scale budgets for convective parameterization. *Mon. Wea. Rev.,* **104,** 1408–1418.

Fuelberg, H. E., and M. F. Printy, 1983: Meso β-scale thunderstorm/environment interactions during AVE-SESAME V (20–21 May 1979). *Bull. Amer. Meteor. Soc.,* **64,** 1144–1156.

——, and ——, 1984: A kinetic energy analysis of the meso β-scale severe storm environment. *J. Atmos. Sci.,* **41,** 3212–3226.

——, M. G. Ruminski and D. O'C. Starr, 1985: Mesoscale generation of available potential energy in the warm sector of an extratropical cyclone. *Mon. Wea. Rev.,* **113,** 1150–1165.

Hudson, H. R., 1971: On the relationship between horizontal moisture convergence and convective cloud formation. *J. Appl. Meteor.,* **10,** 755–762.

Kuo, H. L., 1965: On formation and intensification of tropical cyclones through latent heat release by cumulus convection. *J. Atmos. Sci.,* **22,** 40–63.

——, 1974: Further studies on the parameterization of the influence of cumulus convection on large-scale flow. *J. Atmos. Sci.,* **31,** 1232–1240.

Lewis, J. M., 1975: Test of the Ogura-Cho model on a prefrontal squall line case. *Mon. Wea. Rev.,* **103,** 764–778.

Lin, S. C., and P. J. Smith, 1979: Diabatic heating and generation of available potential energy in a tornado-producing extratropical cyclone. *Mon. Wea. Rev.,* **107,** 1169–1183.

——, and ——, 1982: The available potential energy budget of a severe storm-producing extratropical cyclone. *Mon. Wea. Rev.,* **110,** 521–533.

McNab, A. L., and A. K. Betts, 1978: A mesoscale budget study of cumulus convection. *Mon. Wea. Rev.,* **106,** 764–778.

Maddox, R. A., 1980: Mesoscale convective complexes. *Bull. Amer. Meteor. Soc.,* **61,** 1374–1387.

O'Brien, J. J., 1970: Alternate solution to the classical vertical velocity problem. *J. Appl. Meteor.,* **9,** 193–203.

Orlanski, I., 1975: A rational subdivision of scales for atmospheric processes. *Bull. Amer. Meteor. Soc.,* **56,** 527–530.

Raymond, D. J., and M. Wilkening, 1985: Characteristics of mountain-induced thunderstorms and cumulus congestus clouds from budget measurements. *J. Atmos. Sci.,* **42,** 773–783.

Sienkiewicz, M. E., and J. R. Scoggins, 1982: Moisture processes accompanying convective activity. NASA CR 3542, Marshall Space Flight Center, 86 pp. (Available from Atmospheric Sciences Division, ED-43, Marshall Space Flight Center, AL 35812.)

Spar, J., 1953: A suggested technique for quantitative precipitation forecasting. *Mon. Wea. Rev.,* **81,** 217–221.

Thompson, R. M., Jr., S. W. Payne, E. E. Recker and R. J. Reed, 1979: Structure and properties of synoptic-scale disturbances in the intertropical convergence zone of the eastern Atlantic. *J. Atmos. Sci.,* **36,** 53–72.